Evaluation of Anti Carbapenem-Resistant *Klebsiella Pneumonia* of Zinc Oxide Nanoparticles Synthesized by *Aspergillus Niger* in Vitro and in Vivo

Elsayim Rasha (438203748@student.ksu.edu.sa)
King Saud University
Alkhulaifi Manal
King Saud University
AlOthman Monerah
King Saud University
Ibrahim Khalid
King Saud University
Elnagar Doaa
King Saud University
Khatab Alaa
King Saud University
Manal Awad
King Saud University
Abdalla Mohnad
Shandong University

Research Article

Keywords: KPC, zinc Oxide nanoparticles (ZnO-NPs), X-ray spectroscopy (EDX). re-epithelialisation, antibacterial agents and wound healing.

Posted Date: August 5th, 2021

DOI: https://doi.org/10.21203/rs.3.rs-757409/v1

Abstract

Currently, the mortality rate is increasing in Saudi Arabia's ICU, due to the spread of KPC. This project was carried out to evaluate the ability of the biological synthesized of zinc Oxide nanoparticles (ZnO-NPs) using *Aspergillus niger* to overcome Carbapenem-Resistant *Klebsiella pneumonia* (KPC) in vitro and in vivo. ZnO-NPs was synthesized via a biological method and characterized using UV-Vis spectroscopy, Zeta sizer and Zeta potential analyses, X-ray diffraction (XRD) spectroscopy, Fourier transform infrared spectroscopy (FTIR), scanning electron microscopy (SEM) and energy-dispersive X-ray spectroscopy (EDX). In vitro sensitivity of KPC to ZnO-NPs was identified using the well diffusion method, MIC and MBC was determined by macro dilution method. The morphological alteration of KPC cell after ZnO-NPs treatment was showed by SEM. In vivo susceptibility of KPC to ZnO-NPs ointment was evaluated using wound healing in experimental rats. The chemical characterization findings showed the formation, stability, shape and size of the synthesized nanoparticles. The MIC and MBC results was found in 0.7mg\ml and 1.8mg\ml respectively. in vivo results displayed the inflammation reduction and wound healing re-epithelialisation of kpc infected rats. these findings demonstrated that ZnO-NPs has great potential to be developed as antibacterial agents and wound healing.

1. Introduction

Klebsiella pneumoniae is a Gram-negative, encapsulated, non-motile, rod-shaped opportunistic pathogen. It cause wide range of hospital acquired infections such as: wound infection, bacteremia, pneumonia, and urinary tract infections, particularly in immune compromised people[1].

Klebsiella pneumoniae carbapenemase (KPC)- producing *Enterobacteriaceae* cause infection may associated with the treatment failure and increased mortality[2]. It is increasingly recognized as a serious, worldwide public health concern. That is why is very important to find out new strategies and ecofriendly drug to eradicate KPC and to control this emerging issue of multi drug resistant bacterial strains[3]. Among the genus *Enterobacteriaceae*, carbapenemases are more prevalent in *K. pneumoniae* isolates, which usually causes hospital acquired infections and outbreaks in Saudi Arabia. This is reported by Alotaibi [4]. Also he found that both carbapenem producing *E. coli* and *K. pneumoniae* that isolated from a tertiary care hospital in Riyadh, are more frequently *K. pneumoniae* (63%) compared with *E. coli* (55%)[4].

The international travelling is the primary rout of the spread of KPC spreading in Gulf Cooperation Council (GCC) (Saudi Arabia, United Arab Emirates [UAE], Oman, Kuwait, Qatar, and Bahrain). Theses countries' strong economies have led to the arrival of large numbers of migrants to obtain work and medical care. Also, millions of Muslims visit Saudi Arabia for the Hajj and other religious events every year, which further promotes the spread of KPC[5].

In Saudi Arabia, KPC is high incidence this may due to the large number of Pilgrims, visitors and migrant workers receives from endemic countries such as Turkey, India, and Pakistan every year[6] Survey such as

that conducted by Faiz and M[7] have shown that the incidence of KPC among Makkah hospitals is about 48.4% from other carbapenem producing organisms[7].

Biogenic synthesis of nanoparticles, green synthesis of nanoparticles and biosynthesis of nanoparticles, all of these terms are called to synthesize Nano by using plants or microorganisms. Nanoparticles from such “green synthesis” have been used in the field of drug, gene delivery and various medical treatments including antimicrobial, anticancer, anti-inflammatory, antiaging, antioxidant and anti-biofilm inhibition[8]. Synthesis of oxide nanoparticles by using eukaryotic organism like fungi is good for the synthesis of metal nanoparticles, because of their ability to produce large amount of enzymes [9].

Several attempts have been done to evaluate and experiment the antimicrobial activity of Zinc oxide nanoparticles (Zn-ONPs), On October 2020a group of researcher were studied the antimicrobial activity of biosynthesis Zn-ONPs using aqueous extracts of pomegranate leaves and flowers designated ZnO-NPs-PL, ZnO-NPs-PF. They found that ZnO-NPs were effective against all their selected pathogenic strains including *Klebsiella pneumonia*, then they reported that both ZnO-NPs can effectively be used as alternative antibacterial agents[10]. One study by[11], showed that how ZnO NPs possess strong antimicrobial activity and can promote the antimicrobial activity of some beta-lactam antibiotics such as: *Klebsiella pneumoniae* and *Escherichia coli* [11].

On the side of antimicrobial, ZnO appears to be strong potential to kill microorganisms whereas Zn-ONPs presented strong antibacterial activities on broad-spectrum pathogenic bacteria such as *Bacillus subtilis*, *Staphylococcus aureus*, *Escherichia coli*, *E. coli* O157:H7, *Salmonella enteritidis*, *Salmonella typhimurium*, *Pseudomonas fluorescens*, and *Listeria monocytogenes*. ZnO nanoparticles's mode of action occur through the inhibition of the bacterial growth by fell a part of the cell membrane and increasing the membrane permeability, affect the synthesis of hydrogen peroxide and final penetration of cell wall and disorganization of bacterial membrane[12,13].

2. Results

2.1 Characterization of Zinc oxide nanoparticles synthesized by *Aspergillus niger*

The result of UV-Vis absorbance spectrophotometer (wave range 200–800 nm) of the synthesized Zn-ONPs using *Aspergillus niger* showed an absorbance peak at 304 nm (Fig. 1A). The X-ray diffraction pattern of ZnO-NPs found that the peaks of ZnO-NPs showed at 2θ of 31.77 º, 34.44 º, 36.26 º, 47.55 º, 56.60 º, 62.88 º, 66.38 º, 67.96 º, 69.09 º, 72.98 º, 81.64 º, 92.80 º, 95.32 º and 98.67 º for the (100), (002), (101), (110), (103), (112), (200), (201), (004) and (202) lattice planes respectively (Fig. 1B). To determine the functional groups responsible for the synthesis of ZnO-NPs and to compare the functional group in *Aspergillus niger* which mediate the synthesized nanoparticles before and after calcination we used Furrier Transform Infra-Red Spectroscopy (FTIR) in the range of 400–4000 cm-1. FTIR of ZnO-NPs

according to Fig. 1C, which presented the sharp peak at 3482cm-1 and 3401cm-1 corresponds to O-H strong, group which are found in ZnO-NPs before and after calcination and the aqueous extract of *Aspergillus niger*. ZO group and N-H medium, bend amins group were detected only in ZNO-NPs before calcination. After calcination showed S-H weak, stretching thiol, C = O stretch, α,β-unsaturated aldehyde keton, C-H medium, rock alkanes, C-N medium, stretching aliphatic amins, C-H meadium, wag alkyl halides and C-Br medium, stretching alkyl halides. The previous functional groups in ZnO-NPs after calcination makes it effective against tested bacteria. The aqueous extract of *Aspergillus niger* have several functional groups which responsible of the synthesized of zinc oxide nanoparticles such as: C = O, C-C, C-N, C-Cl) and C-Br groups.

The measured zeta potential value of biosynthesized zinc oxide nanoparticles showed in Fig.2A&B, were foundmean Z-average diameter (nm) of the ZnO-Nps and the size distribution were observed to be 176.5nm for zeta size and −0.734mV for zeta potential. The size distribution profile was 100% and 0%.**Figure 2. (A)** Zetasizer of ZnO-NPs. (**B**) Zeta potential of ZnO-NPs.

The results of SEM and EDX was conducted to confirm the formation of nanoparticles and their elemental composition, SEM is also analyze the structure of ZnO-NPs that were formed. SEM image of Fig. 3B, has shown an irregular, individual spherical shape, and most of them presented with aggregates hexagonal shape with a smooth surface and were apparently devoid of cracks. The elemental analysis of ZnO-NPs for Zinc and Oxygen components showed 61.63% zinc and 38.37% oxygen Fig. 3A.

2.2 Antibacterial activity:

Interestingly, the zone of inhibition (ZOI) results was observed promising outcoms of the synthesized ZnO-NPs against tested bacteria (KPC) using an agar well diffusion method. All tested KPC and *Klebsiella pneumoniae* (ATCC700603) as control were showed highly sensitivity to ZnO-NPs (20.8 ± 20.8 ± 2.7mm) at 7.5 mg\ml concentration, (Fig. 4A). The minimum inhibitory concentration (MIC) was determined by the macro dilution method in culture broth followed by the minimum bactericidal concentration by the agar dilution method. Figure 4B,C &D and Table 1, presented the experimental data of MIC and MBC for all tested KPC; the mean score for MIC was 0.7 mg/ml and for MBC was 1.8 mg/ml.

Table 1
Comparison between MIC and MBC.

	MIC	MBC
Mean ± Std. Deviation	**0.7 ± 1.79**	**1.8 ± 1.56**

2.3 SEM for bacterial cell morphology

The bacterial cell morphology changes were studied by SEM. From the Fig. 3C, D&E, we can see that KPC cell treated with ZnO-NPs reported significantly changes in the bacterial cell included severe damage, change and decreased in size shape from rod-shaped to slightly coccus-shaped, also showed multiple dents on the cell surface these results. Whereas, the untreated KPC cells and those treated with impenem have no morphological change was reported. The findings from SEM are matching with those[14–16].

2.4 ZnO-NPs improves KPC-infected wound healing in rats

Wound healing evaluation was based on the change of fresh wounds of rats and the degree of closure on days 3, 7, 11, and 14 after wounding (Fig. 5). Group-1 (G-1), the infected and untreated control group showed severe tissue inflammation with

purulence on the wound surface on all days. Group-2 (G-2), the infected and untreated control group showed tissue inflammation on day-3,7 and 11, with slight

bleeding on day-7. Group-3 (G-3), the infected and treated with imipenem ointment group showed sever inflammation on day-3, 7 and 11 with slight bleeding thick mixture of layers of organisms and purulence, while on day-14 the tissue recovered the damage and inflammation. Group-4 (G-4), the infected and treated with ZnO-NPs ointment, showed severe tissue inflammation with slight bleeding on day-3 and 7, which disappeared on day-11 with significant improvement of healing on day-14. Statistical analyses of the mean percentage of wound healing on day 14 after wounding showed that G-1 displayed comparable wound heal rate (63%) healing with G-2 (64%) healing, while, G-3 exhibited moderate result (70%) healing and G-4 presented promising result (96%) (Table 2. A histogram of Table 2 is shown in Fig. 4E).

Table 2
The percentage of mean wound recovery in wound area within 14 days of wounding in

Groups	Days			
	3rd Day in%	7th Day in%	11th Day in%	14th Day in%
Group 1	7 ± 2.739	17 ± 2.739	30 ± 5.000	63 ± 5.701
Group 2	10 ± 5.000	18 ± 6.708	30 ± 7.071	64 ± 9.618
Group 3	10 ± 3.536	39 ± 8.944	54 ± 4.183	70 ± 6.124
Group 4	7 ± 2.739	60 ± 5.000	85 ± 5000	96 ± 2.236

2.5 General histopathology of wound healing

Hematoxylin and eosin (H&E) used to stained the stages of wound healing from the four groups of rats under investigation on days 3, 7, and 14. Unwounded control skin posted normal skin feature with

epidermis layer of stratified squamous epithelia thickened (348 μm) sheathed with keratinized layer and underneath with dermis layer of connective tissue (Fig. 6A). Untreated wounded skin after 3 days of post operation day (POD) altered hemorrhage and granulomatous reaction of inflammatory cells (Fig. 6B). Whereas, untreated infected wounded skin revealed more granulomatous reaction 3 days of POD (Fig. 6C).

Untreated wounded skin after 7 days of POD represented a primary formation of scab underneath with inflammatory granulomatous reaction (Fig. 7A). While, infected untreated wounded skin showed heavy incidence of hemorrhage foci and inflammation (Fig. 7B). Moreover, infected wound skin treated with Imipenem antibiotic exhibited formation of scab and inflammation (Fig. 7C). Furthermore, infected wound and treated with ZnO-NPs also showed more scab formation and granulomatous reaction (Fig. 7D).

Untreated wounded skin 14 days post to wound cut displayed a superficial scab to inflammatory granulomatous reaction (Fig. 8A). Whereas, infected untreated wounded skin showed more concentrated inflammation beneath the scab (Fig. 8B). Additionally, infected wound treated with Imipenem antibiotic showed thickened regenerated epidermis (710μm) sheathed with keratinized layer (Fig. 8C). Furthermore, infected wound and treated with ZnO-NPs posted marked improvement of wound with regenerated differentiate epidermis (391μm) and more improved dermis (Fig. 8D).

3. Discussion

An initial objective of this project was to find out and develop new antibacterial agent to manage bacterial infections which occur due to KPC. The current study found that the *Aspergillus niger* mediate the biological synthesis of ZnO-NPs was appeared promising activity against KPC, also the most interesting finding was that shows in the recovery of wounds, this may due to the stability of the synthesized nanoparticles for long time. In reviewing the literature, no more in vivo studies was found. Optical properties of ZnO-NPs were characterized using UV–Vis spectrophotometer. Zinc oxide formation was confirmed as the absorption peak (lambda max) was found near 304 nm. This result correlate with the result which reported by Aldalbahi[17], who was observed the maximum peaks of ZnO NPs at 300 and 359 nm. The results of UV-Vis were confirmed the present of ZnO-NPs. The measured zeta potential value of ZnO-NPs possesses a negative zeta potential value of -0.734 mv, which indicated that these nanoparticles have a high stability due to the electrostatic repulsive force[18]. For zeta sizer, ZnO-NPs showed (176nm) in size. The XRD results are consistent with those of [15,19], Although, these results differ from some published studies[17]. On the side of nanoparticles structure, ZnO-NPs showed a crystalline hexagonal structure similar to the synthesized nanoparticles structure reported by [15,20]. XRD indicates that the synthesized nanoparticles are in their purest form and have a crystalline structure. A possible explanation for these results due to their tight and strong diffraction peaks. To identified the various functional groups found in synthesized nanoparticles and the aqueous extract of *Aspergillus niger* as control were characterized under FTIR. The functional group O-H was presented in the aqueous extract of *Aspergillus niger* and ZnO-NPs before and after calcination, this result explain that O-H group is the

reducing agent which responsible of ZnO-NPs formation. While most of the functional groups detected as shown in Fig. 1C, such as C-H, C = O, C-C, N-H, N-O, C-N, OH, and ZnO, were similar to those obtained previous [21–23]. Size and the morphology of the ZnO-NPs were identified using the SEM. The average particle size was around 48–88 nm, with a hexagonal shape, this study produced results which corroborate the findings of a great deal of the previous work in SEM image [24–26]. Interestingly, ZnO-NPs was found to have a promising antibacterial activity, ZOI mean for the tested KPC was 20.8 mm vis 22.9 for the ATCC [27]. This finding corroborates the results of many researchers who obtained 16–27 mm of ZOI [11,20,28,29].

According to Van vuuren [30], and others natural products with MIC values below 1.0 mg/ml are considered noteworthy. The mean MIC and MBC of ZnO-NPs was 0.7mg\ml, 1.8 mg\ml respectively, It is encouraging to compare this result with that found by Yousef and others[20], Their MIC result was 500 mg/mL against *Bacillus subtilis*, *Bacillus megaterium*, *Sarcina lutea*, *Klebsiella pneumoniae*, and Proteus vulgaris. This result is confirmed that the biosynthesis of nanoparticles is better than other method of synthesis. Nonetheless, ZnO-NPs achieved high stability and potency as antibacterial, according to the MIC and MBC result's. SEM analysis assists in the prediction that ZnO-NPs that interact with KPC surface may lead to transformations in cell size and shape these changes resulted to the disruption of the cell membrane and the death of the cell[23]. Surprisingly, in the side of in vivo experiments, the fresh wound healing area was found to have a promising result in G-4, which treated with ZnO-NPs ointment, while G-3 showed moderate healing it seems possible that these results are due to the resistance of the tested bacteria to Imipenem and G-1 and G-2 were presented the lowest wound healing, this may due to their dependent to the recovery of immune response only.

4. Methodology

4.1 Synthesis of ZnO-NPs by using *Aspergillus species*:

The biosynthesis of nanoparticles by *Aspergillus niger* was modified from two references to develop the stability of the synthesized nanoparticles. *Aspergillus niger* (ATCC 16404 NA) was obtained from mycology department, King Khaled Hospital and inoculated aerobically in Czepak Dox agar plate for 96 hours at room temperature in orbital shaker at 160 rpm. The fungal biomass was harvested by Whatman no.1 filter paper to collect free fungal filtrate. Then the filtrate was washed by centrifuge at 10.000 rpm for 20 min, after that was transferred to 250 ml sterile flask and mix with 200ml of deionized water and incubated at room temperature in shaker incubator for 72 h at 200 rpm. Then, filtrated by Whatman no.1 filter paper and collected the filtrate of *Aspergillus niger*. To prepared zinc oxide nanoparticles we prepared 100 ml of 0.25 mM solution of zinc nitrate and added to 10 ml of *Aspergillus niger* filtrate and incubated in shaker incubator at 180 rpm for one week at 37^{o}c. Finally, white to yellow paste of ZnO-Nps were formed as showed in Fig. 9, then, packed it until used[31,32].

4.2 The synthesized ZnO-NPs Characterization

The formation of ZnO-NPs was confirmed by UV-vis spectroscopy (UV-1800; Shimadzu UV Spectrophotometer, Kayoto, Japan), with the wave length range of 200–800 nm at resolution of 10nm. The zeta sizer and potential measurement was performed using dynamic light scattering and Malvern Zetasizer nanoseries compact scattering spectrometer (Malvern Instruments Ltd. Malvern, UK) respectively, the histogram was developed by Zetasizer software (version 7.11) (Malveren Panalytical, Malveren, UK). Zeta potential was measured by using the folded capillary cell of Malvern. Fourier Transform Infra-Red Spectroscopy (FTIR) was recorded in the range of 400–4000 cm-1 Nicolet (Parkin Elmer, Spectrum BX, Waltham, UK). To identify and determine the different functional groups present in the *Aspergillus niger* filtrate before and after mixed with Zinc nitrate, and the synthesized ZnO-NPs. The structure and crystalline nature and composition of synthesized ZnO NPs was analyzed by X-Ray diffraction (XRD). The formation, symmetry, size and shape of nanoparticles were analyzed in the form of powdered by an X-Ray diffractometer (Brucker-Discover D8, CUK-alpha, Sangamon Ave, Gibson, USA) of 2 /min scan speed the range 10–100∘.Scanning electron microscopy (SEM) analysis was done to measure the size and the composition of synthesized nanoparticles using SEM (JEOL model, JSM-761OF, Tokyo, Japan) operated at an accelerating voltage of 10 kV with an EDX detector SEM machine. small amount of dry ZnO-NPs was prepared as thin film on a carbon coated copper grid, then dried the film by putting it on the SEM grid under a mercury lamp for five minutes.

4.3 In vitro microbial susceptibility testing of the synthesized ZnO-NPs

Microbial susceptibility testing was performed by agar well diffusion technique. Tested bacteria (carbapenemase- producing *Klebsiella pneumoniae* (KPC)) were isolated as a retrospective sample from wounds of ICU patients at Prince Mohammed Bin Abdul Aziz Hospital - Al Madinah. Then, all samples were identified in microbiology department in the hospital by using VITEK 2 systems version: 08.01. *Klebsiella pneumoniae* (ATCC 700603) was tested as control and was obtained from the College of Applied Medical Science, King Saud University. All bacterial samples were kept in Nutrient Agar slant (NA) and stored at 4^0c until used[33]. well plate agar diffusion method, was carried out by inoculated the tested bacteria on nutrient broth overnight, and adjusted to 0.5 McFarland turbidity standards, then each bacteria streaked on a Mueller–Hinton agar (MHA) plate by swab. A sterile cork borer was used to form wells (6 mm in diameter) on the agar plates. Then, we added 7.5 mg of ZnO-NPs dissolved in 1 mL of deionized water to obtain a concentration of 7.5 mg/mL, and add 0.5 ml of ZnO-NPs to each well in the inoculated culture plates and incubated at 37^oc overnight [26]. The microbial susceptibility was determined by measuring zoon of inhibition (ZOI) twice. Minimum Inhibitory Concentration (MIC), was done by the broth macro dilution method according to the CLSI[27]. Minimum Bactericidal Concentration (MBC), was performed by obtaining loop full from MIC tubes which did not show any visible growth and inoculated on sterile Mueller–Hinton agar. The MBC result was recorded in the concentration which no visible growth was seen[21].

4.4 Scanning Electron Microscopy technique for Bacterial Samples images

Scanning electron microscopy (SEM) was carried out for KPC cells untreated (negative control), treated with Imipenem (Positive control) and treated with ZnO-NPs (tested sample) to study the morphological cell alterations. The treated cells of KPC were fixed with 2.5% glutaraldehyde in a phosphate buffer having pH 7.2. The samples were post-fixed in 1% osmium tetroxide, followed by dehydration through an ascending ethanol series, critical point dried and coated with Au–Pd (80:20) using a Polaron E5000 sputter coater, Quorum Technologies, Laughton, UK. The samples were checked at an accelerating voltage of 25 kV in FEI Quanta 250 using an SE detector[34,35].

4.5 In vivo KPC susceptibility for ZnO-NPs

All procedures including animals were approved by the Animal Care and Use Committee at King Saud University (Ethics Reference Number: KSU-SE-1978). Male Sprague–Dawley (SD) rats aged 12–14 weeks old were obtained from the Animal House of the College of Pharmacy, King Saud University, Riyadh, Saudi Arabia. Rats were anesthetized in accordance with the guidelines published by the University of California San Francisco, Office of Research Institutional Animal Care and Use. All methods were performed in accordance with the relevant guidelines and regulations. All animal experiments were conducted in compliance with the ARRIVE guidelines. Two cm of thickness cutaneous incisions were made on the dorsal area of rats under anesthesia (100 mg ketamine/kg of body weight and 5 mg xylazine/kg of body weight)[34,36]. The experimental rats were divided to four groups each group have five rats, **G-1 wounded, infected** with KPC and **un treated** (positive control), **G-2 wounded, uninfected with KPC and untreated** (negative control), **G-3 wounded, infected with KPC and treated with Imipenem and G-4** wounded, infected with KPC and treated with ZnO-NPs ointment[34]. To avoid the cross-infection or manipulation of Rat's wound, we placed each rat in a separate cage. The treatment of wounded rats was starting since day 3 of post operation. Measurement of wound area was determined on Post operation day 3, 7, 11, and 14[36,37]. The macroscopic images of the wound site were taken on day 3, 7, 11 and 14 by Huawei mate-9 Came. At day 14, the rats were sacrificed by physical method (carbon dioxide inhalation) after filled the chamber with carbon dioxide for several minutes, and the skin tissues of the wound site were collected at day 3, 7 and 11 by chosen one rat from each group and under weak anesthesia we collected the skin samples to avoid any pain during the collection. While, at day 14 the samples collected after sacrificed all rat's groups. Hematoxylin and eosin (H&E) staining were performed for the histological analysis[38] (Fig. 10). Tissue sections were checked under a light microscope (Nikon, Eclipse i80), and images were taken at different magnifications using a Nikon mounted digital camera (OXM 1200C; Nikon, Japan).

4.6 Preparation of gel based ointments

Equal volumes of polyethylene glycol (PEG) 400–2000 was added to ZnO-NPs and imipenem separately, followed by boiling them at 65 _C for 5 min Ointment formulations to prepared 5 mg/mL of the oinment[39].

3.6 Statistical analysis

Statistical analysis of the rate of wound recovery was performed using multivariate analysis of variance, and the statistical analysis of MIC, MBC, and ZOI was performed using paired samples t-test and ANOVA, with the results presented as mean ± SD with SPSS statistical software version 22 (SPSS Inc., Chicago, IL, USA).

5. Conclusion

This project was undertaken to design new way to treat the Carbapenem-Resistant *Klebsiella pneumonia* and evaluate the activity of it in vitro and in vivo. In this study we showed promising results in both in vivo and in vitro and we found that there was a correspondence between in vitro and in vivo results. The chemical characterization results of this study indicate that, the biological synthesis of nanoparticles provided nanoparticles with small size, suitable shape, stable for long time and have antibacterial activity. UV-Vis showed 304 nm which confirmed the formation of ZnO-NPs. XRD and zeta potential results presented the purity and the crystalline form of ZnO-NPs. O-H functional group was playing significant role in the formation of ZnO-NPs, according to the FTIR findings. Zeta sizer found that the size of ZnO-NPs was 176nm and EDX result was detected the components of the synthesized ZnO-NPs which appeared 61.63% for Zinc and 38.37% for the Oxygen. The MIC of ZnO-NPs was 0.7 mg\ml and MBC was 1.8 mg\ml with 20.8mm of ZOI. ZnO-NPs ointment presented interesting results in wound healing, these results support the aim of this study of using ZnO-NPs as antibacterial agent.

6. Declarations

Competing interest

The authors declare no competing interests.

Author contribution

Conceptualization, Alkhulaifi Manal (A.M.) and ElsayimRasha (E.R).; Data curation, E.R.; Funding acquisition, AlOthman Monerah (A.M.); Investigation, A.M; Methodology, E.R, Elnagar Doaa (E.D), Ibrahim Khalid (I.K), Awad.A.Manal (M.A.A.) and Khataab Alaa (K.A).; Supervision, AlOthman Monerah (A.M.); Writing–original draft, E.R., Abdulla Mohnad (M.A) and E.D.; Writing–review and editing, M.A.

Data Availability

Not applicable

Acknowledgment

The authors would like to thank the Deanship of Scientific Research in King Saud University for funding and supporting this research through the initiative of DSR Graduate Students Research Support (GSR). The authors also extend their sincere appreciation to Dr. Manal Awad for her guidance in Nano synthesis part also we thank Abdullrahman Salih and Tayseer Almeneazel for their help in this project by providing materials.

7. References

1. Rani, R., Sharma, D., Chaturvedi, M. & JP, Y. Green Synthesis, Characterization and Antibacterial Activity of Silver Nanoparticles of Endophytic Fungi Aspergillus terreus. *J. Nanomed. Nanotechnol.***08**, (2017).
2. Toledo, P. V. M. *et al.* Activity of antimicrobial combinations against KPC-2-producing Klebsiella pneumoniae in a rat model and time-kill assay. *Antimicrob. Agents Chemother.***59**, 4301–4304 (2015).
3. Padalia, H., Moteriya, P. & Chanda, S. Green synthesis of silver nanoparticles from marigold flower and its synergistic antimicrobial potential. *Arab. J. Chem.* (2015) doi:10.1016/j.arabjc.2014.11.015.
4. Alotaibi, F. Carbapenem-Resistant Enterobacteriaceae: An update narrative review from Saudi Arabia. *J. Infect. Public Health***12**, 465–471 (2019).
5. Sonnevend, Á., Ghazawi, A. A., Hashmey, R. & Jamal, W. Characterization of Carbapenem-Resistant Enterobacteriaceae with High Rate of Autochthonous Transmission in the Arabian Peninsula. 1–14 (2015) doi:10.1371/journal.pone.0131372.
6. Liao, J., Xu, G., Mevers, E. E., Clardy, J. & Watnick, P. I. A high-throughput, whole cell assay to identify compounds active against carbapenem-resistant Klebsiella pneumoniae. *PLoS One***13**, 1–20 (2018).
7. Aftab Faiz, M. A. K. Frequency of Carbapenemase Producing Klebsiella pneumoniae in Makkah, Saudi Arabia. *J. Microbiol. Infect. Dis.***6**, 121–121 (2016).
8. Castro-Aceituno, V. *et al.* Anticancer activity of silver nanoparticles from Panax ginseng fresh leaves in human cancer cells. *Biomed. Pharmacother.* (2016) doi:10.1016/j.biopha.2016.09.016.
9. Castro-Longoria, E., Vilchis-Nestor, A. R. & Avalos-Borja, M. Biosynthesis of silver, gold and bimetallic nanoparticles using the filamentous fungus Neurospora crassa. *Colloids Surfaces B Biointerfaces* (2011) doi:10.1016/j.colsurfb.2010.10.035.
10. Ifeanyichukwu, U. L., Fayemi, O. E. & Ateba, C. N. Green Synthesis of Zinc Oxide Nanoparticles from Pomegranate (Punica granatum) Extracts and Characterization of Their Antibacterial Activity. *Molecules***25**, 4521 (2020).
11. R, F. *et al.* Antimicrobial Behavior of Zinc Oxide Nanoparticles and β-Lactam Antibiotics against Pathogenic Bacteria. *Arch. Clin. Microbiol.***08**, 1–5 (2017).
12. Huh, A. J. & Kwon, Y. J. 'Nanoantibiotics': A new paradigm for treating infectious diseases using nanomaterials in the antibiotics resistant era. *Journal of Controlled Release* (2011) doi:10.1016/j.jconrel.2011.07.002.

13. Ravushankar, R. & Jamuna, B. Nano AB.pdf. *cience against Microb. Pathog. Commun. Curr. Res. Technol. Adv. A. Méndez-Vilas* (2011).
14. Hameed, A. S. H. *et al.* In vitro antibacterial activity of ZnO and Nd doped ZnO nanoparticles against ESBL producing Escherichia coli and Klebsiella pneumoniae. *Sci. Rep.***6**, 1–11 (2016).
15. Liu, S. *et al.* Assessment of antimicrobial and wound healing effects of Brevinin-2Ta against the bacterium Klebsiella pneumoniae in dermally-wounded rats. *Oncotarget***8**, 111369–111385 (2017).
16. Sharma, N. *et al.* Preparation and evaluation of the ZnO NP–ampicillin/sulbactam nanoantibiotic: Optimization of formulation variables using RSM coupled GA method and antibacterial activities. *Biomolecules***9**, (2019).
17. Aldalbahi, A. *et al.* Greener Synthesis of Zinc Oxide Nanoparticles: Characterization and Multifaceted Applications. *Molecules***25**, 1–14 (2020).
18. Chaudhuri, S. K. & Malodia, L. Biosynthesis of zinc oxide nanoparticles using leaf extract of calotropis gigantea: Characterization and its evaluation on tree seedling growth in nursery stage. *Appl. Nanosci.***7**, 501–512 (2017).
19. Bancroft, J. D. & Layton, C. *Connective and other mesenchymal tissues with their stains*. *Bancroft's Theory and Practice of Histological Techniques* (2019). doi:10.1016/b978-0-7020-6864-5.00012-8.
20. M. Yousef, J. & N. Danial, E. In *Vitro* Antibacterial Activity and Minimum Inhibitory Concentration of Zinc Oxide and Nano-particle Zinc oxide Against Pathogenic Strains. *Int. J. Heal. Sci.***2**, 38–42 (2012).
21. Senthilkumar, S. R. & Sivakumar, T. Green tea (Camellia sinensis) mediated synthesis of zinc oxide (ZnO) nanoparticles and studies on their antimicrobial activities. *Int. J. Pharm. Pharm. Sci.***6**, 461–465 (2014).
22. Gautam, S. Developing ZnO Nanoparticle embedded Antimicrobial Starch Biofilm for Developing ZnO Nanoparticle embedded Antimicrobial Starch Biofilm for Food. (2019).
23. Kavitha, S., Dhamodaran, M., Prasad, R. & Ganesan, M. Synthesis and characterisation of zinc oxide nanoparticles using terpenoid fractions of Andrographis paniculata leaves. *Int. Nano Lett.***7**, 141–147 (2017).
24. Siddiquah, A. *et al.* Exploiting in Vitro potential and characterization of surface modified zinc oxide nanoparticles of Isodon Rugosus extract: Their clinical potential towards hepg2 cell line and human pathogenic bacteria. *EXCLI J.***17**, 671–687 (2018).
25. Alamdari, S. *et al.* Preparation and characterization of zinc oxide nanoparticles using leaf extract of sambucus ebulus. *Appl. Sci.* (2020) doi:10.3390/app10103620.
26. Safawo, T., Sandeep, B. V., Pola, S. & Tadesse, A. Synthesis and characterization of zinc oxide nanoparticles using tuber extract of anchote (Coccinia abyssinica (Lam.) Cong.) for antimicrobial and antioxidant activity assessment. *OpenNano***3**, 56–63 (2018).
27. *Methods for Dilution Antimicrobial Susceptibility Tests for Bacteria That Grow Aerobically; Approved Standard — Ninth Edition*. vol. 32 (2012).

28. Sharma, R. *et al.* Polymyxin B in combination with meropenem against carbapenemase-producing Klebsiella pneumoniae: pharmacodynamics and morphological changes. *Int. J. Antimicrob. Agents***49**, 224–232 (2017).
29. Jesline, A., John, N. P., Narayanan, P. M., Vani, C. & Murugan, S. Antimicrobial activity of zinc and titanium dioxide nanoparticles against biofilm-producing methicillin-resistant Staphylococcus aureus. *Appl. Nanosci.***5**, 157–162 (2015).
30. van Vuuren, S. F. & Viljoen, A. M. In vitro evidence of phyto-synergy for plant part combinations of Croton gratissimus (Euphorbiaceae) used in African traditional healing. *J. Ethnopharmacol.***119**, 700–704 (2008).
31. Kalpana, V. N. *et al.* Biosynthesis of zinc oxide nanoparticles using culture filtrates of Aspergillus niger: Antimicrobial textiles and dye degradation studies. *OpenNano***3**, 48–55 (2018).
32. Rajan, A., Cherian, E. & Baskar, G. Biosynthesis of Zinc Oxide Nanoparticles using Aspergillus fumigatus JCF and its Antibacterial Activity. *Int. J. Mod. Sci. Technol.***1**, 52–57 (2016).
33. Sharada S, O. V. Green Synthesis and Characterization of Silver Nanoparticles and Evaluation of their Antibacterial Activity using Elettaria Cardamom Seeds. *J. Nanomed. Nanotechnol.***06**, 2–5 (2015).
34. Kelly, A. M., Mathema, B. & Larson, E. L. International Journal of Antimicrobial Agents Carbapenem-resistant Enterobacteriaceae in the community : a scoping review. *Int. J. Antimicrob. Agents***50**, 127–134 (2017).
35. Kim, K. M. *et al.* Physicochemical properties of surface charge-modified ZnO nanoparticles with different particle sizes. *Int. J. Nanomedicine***9**, 41–56 (2014).
36. Siddiquah, A. *et al.* Exploiting in Vitro potential and characterization of surface modified zinc oxide nanoparticles of Isodon Rugosus extract: Their clinical potential towards hepg2 cell line and human pathogenic bacteria. *EXCLI J.* (2018) doi:10.17179/excli2018-1327.
37. Sivaranjani, V. & Philominathan, P. Synthesize of Titanium dioxide nanoparticles using Moringa oleifera leaves and evaluation of wound healing activity. *Wound Med.***12**, 1–5 (2016).
38. Zowawi, H. M. *et al.* Molecular Characterization of Carbapenemase-Producing Escherichia coli and Klebsiella pneumoniae in the Countries of the Gulf Cooperation Council : Dominance of OXA-48 and NDM Producers. **58**, 3085–3090 (2014).
39. Tiwari, V. *et al.* Mechanism of anti-bacterial activity of zinc oxide nanoparticle against Carbapenem-Resistant Acinetobacter baumannii. *Front. Microbiol.***9**, 1–10 (2018).

Figures

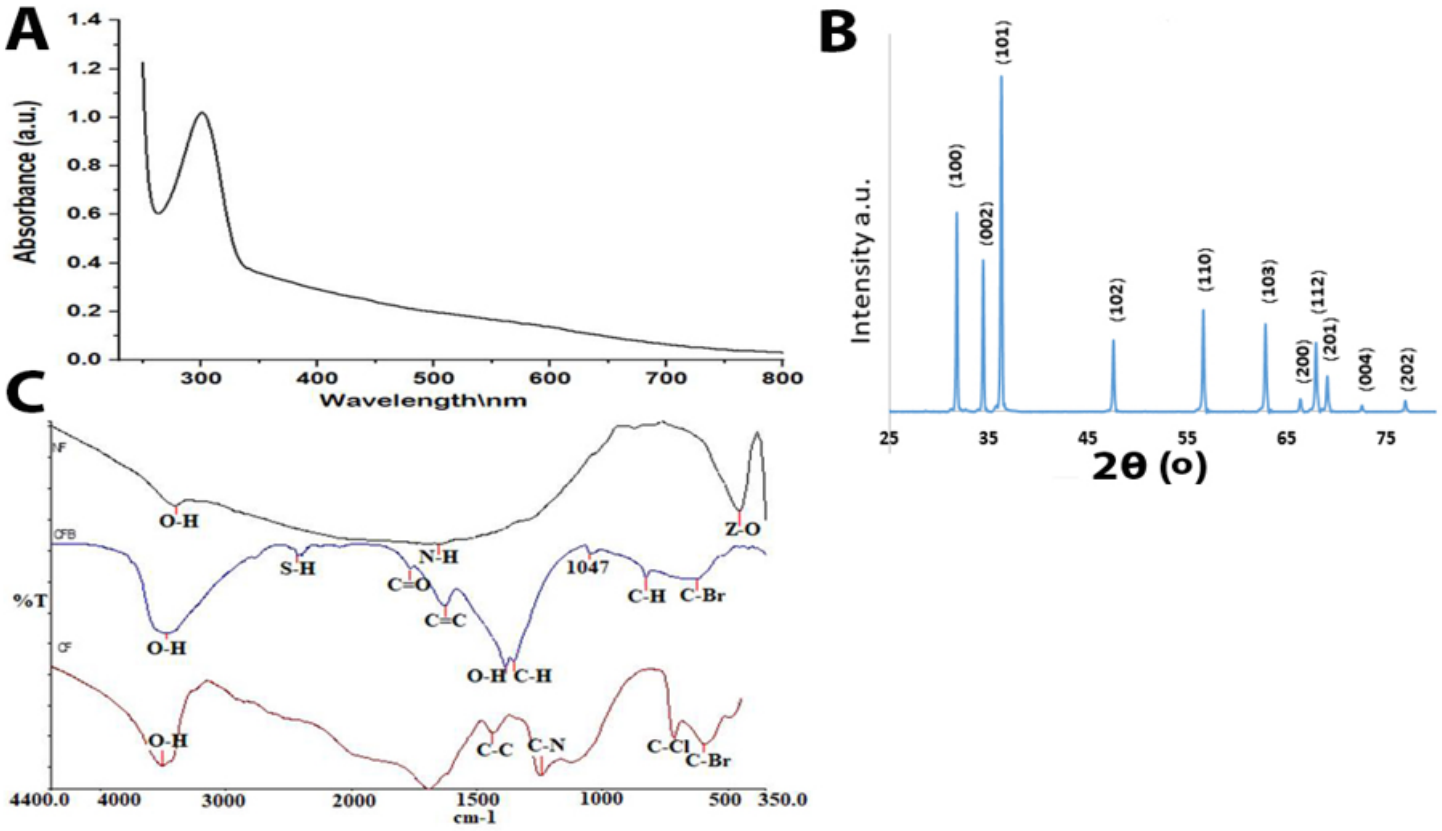

Figure 1

(A) UV–visible spectra of ZnO-NPs. (B) XRD of ZnO-NPs. (C) FTIR of ZnO-NPs.

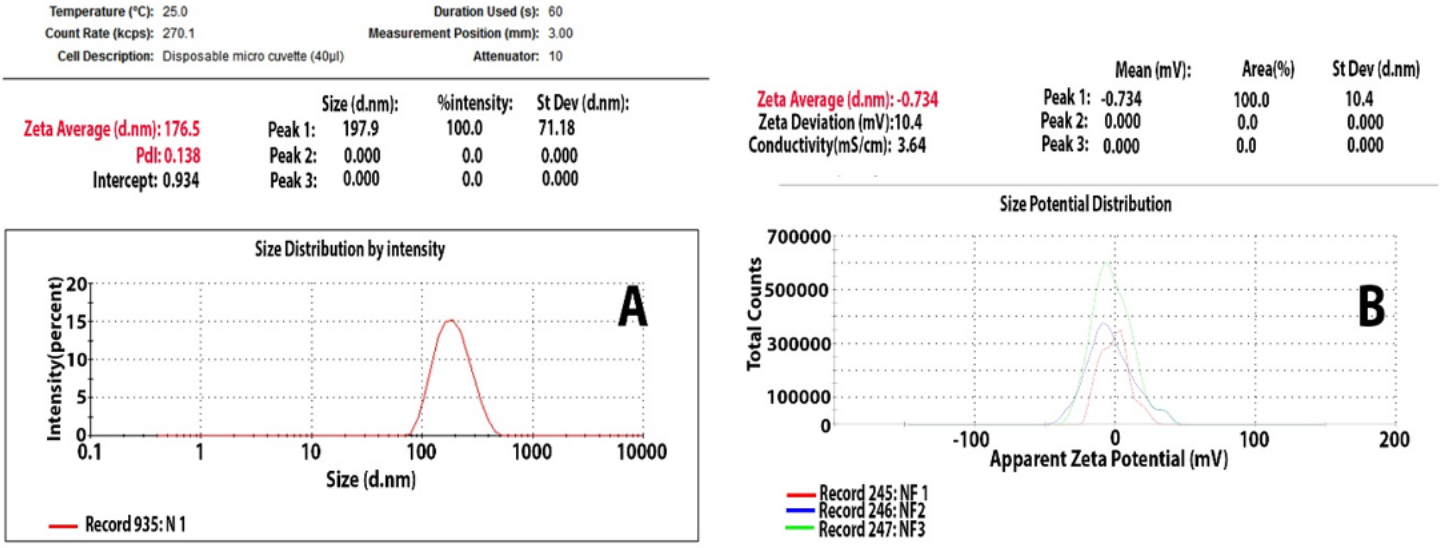

Figure 2

(A) Zetasizer of ZnO-NPs. (B) Zeta potential of ZnO-NPs.

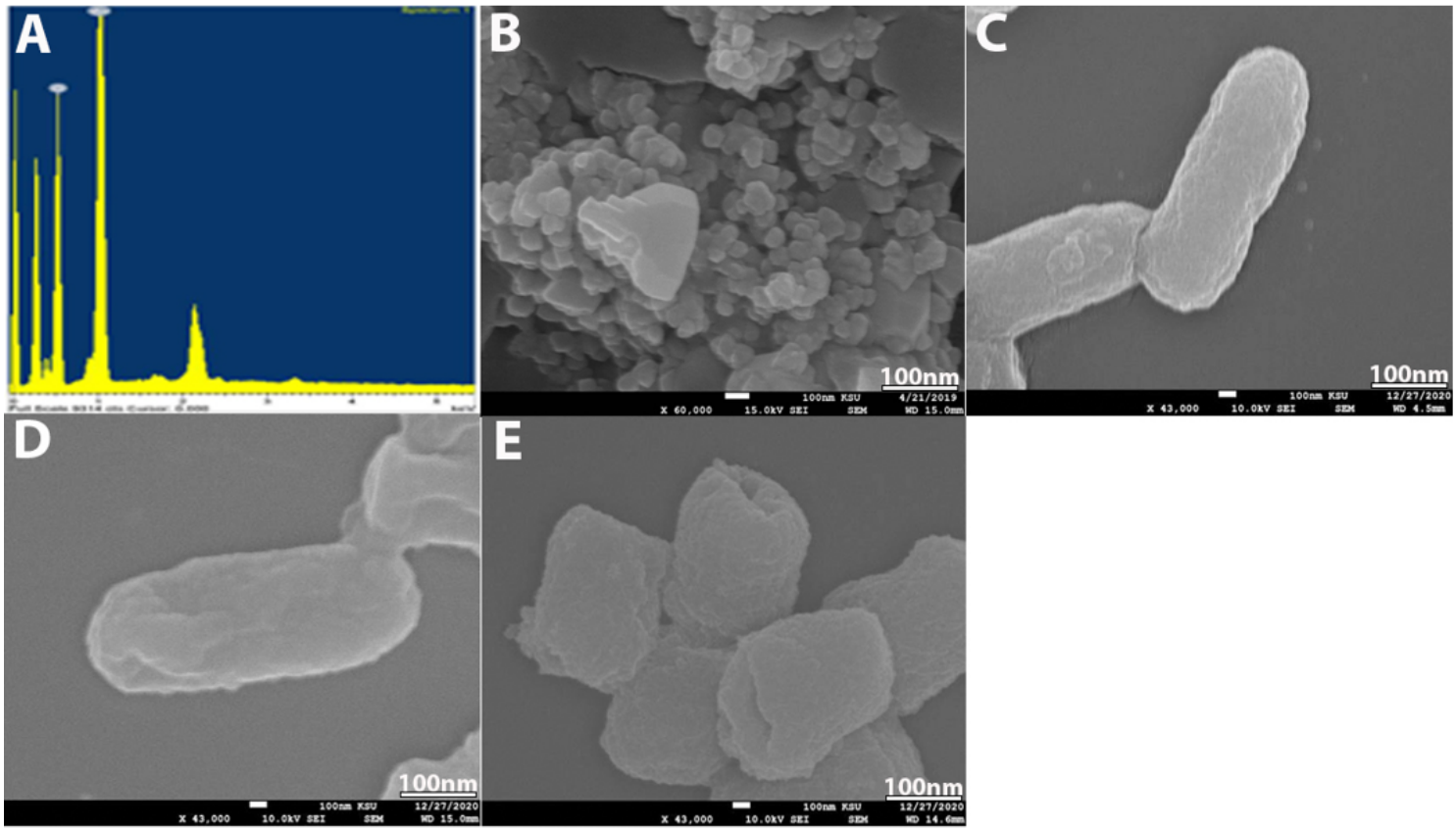

Figure 3

(A) EDX analysis of ZnO-NPs. (B) SEM image of ZnO-NPs. (C) SEM of bacterial control. (D) KPC treated with imipenem at 500 mg/mL. (E) KPC treated with ZnO-NPs.

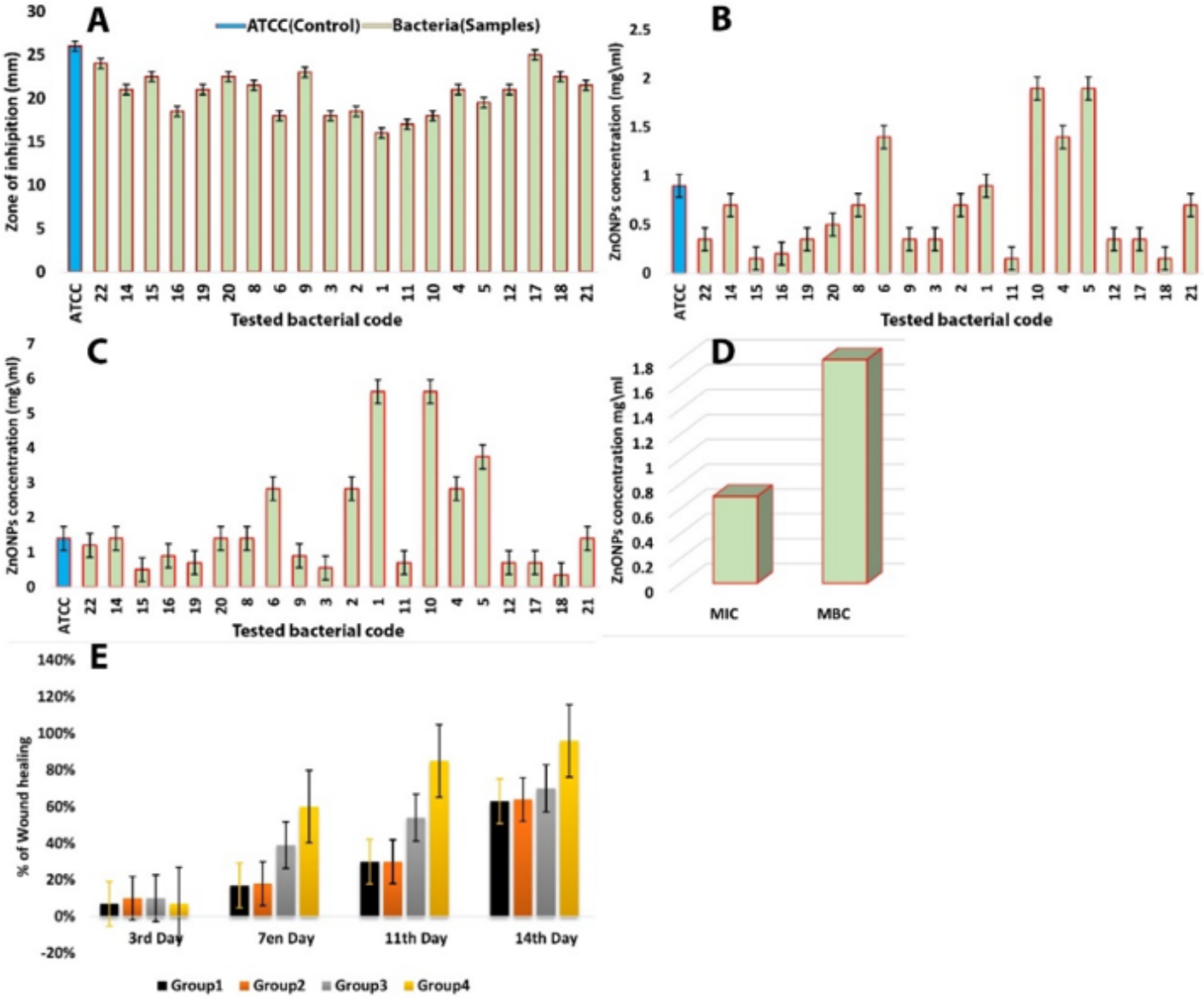

Figure 4

(A) Zone of inhibition (mm) of ZnO-NPs against Klebsiella pneumoniae (ATCC 700603) and KPC bacteria. (B) MIC of ZnO-NPs against KPC and Klebsiella pneumoniae (ATCC 700603). (C) MBC of ZnO-NPs against KPC and Klebsiella pneumoniae (ATCC 700603). (D) Comparison between MIC and MBC.The percentage of mean. (E) wound recovery in wound area within 14 days of wounding in Group 1 (infected and untreated control), Group 2 (infected and untreated control), Group 3 (infected and treated with imipenem),and Group 4 (infected and treated with ZnO-NPs).

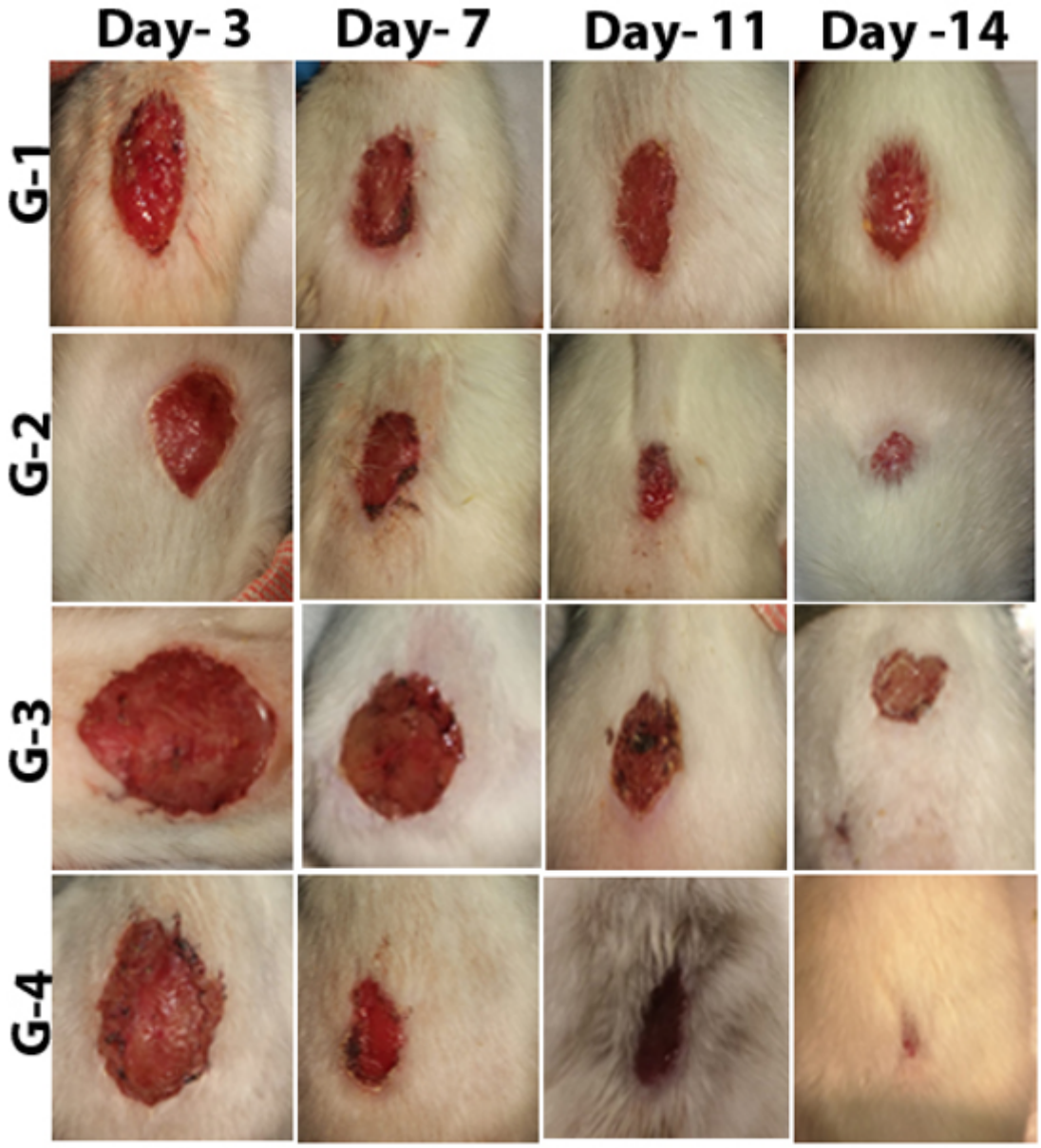

Figure 5

The stages of wound recovery in wound area within 14 days of wounding in Group G-1 (infected and untreated control), Group G-2 (uninfected and untreated control), Group G-3 (infected and treated with imipenem), and Group G-4 (infected and treated with ZnO-NPs).

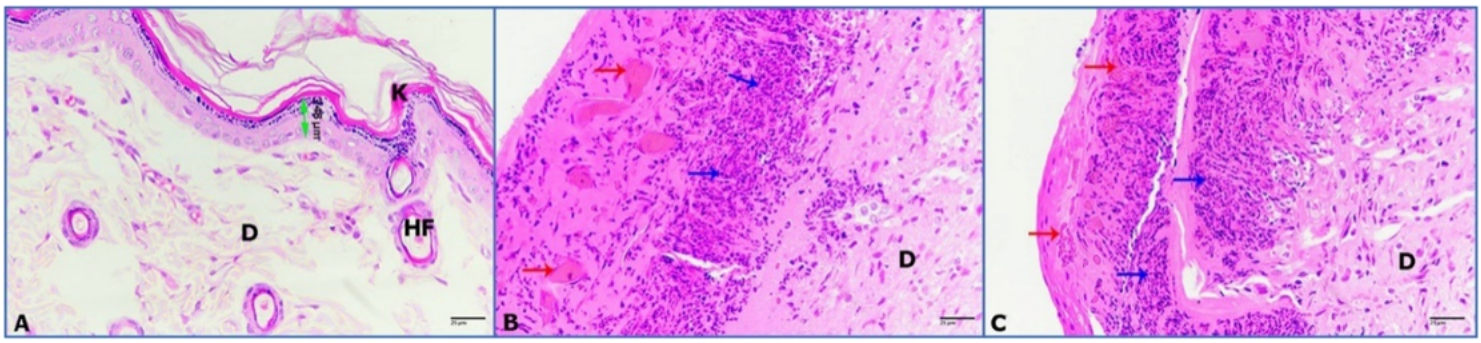

Figure 6

Photomicrographs of rat skin on day-3 , (K) keratinized layer , (D) dermis , (HF) hair follicle , (double head arrow) epidermis , (red arrows) hemorrhage , (blue arrows) granulomatous reaction. (A) Control skin, (B) untreated wounded skin , (C) untreated infected wounded skin . (HE-400X).

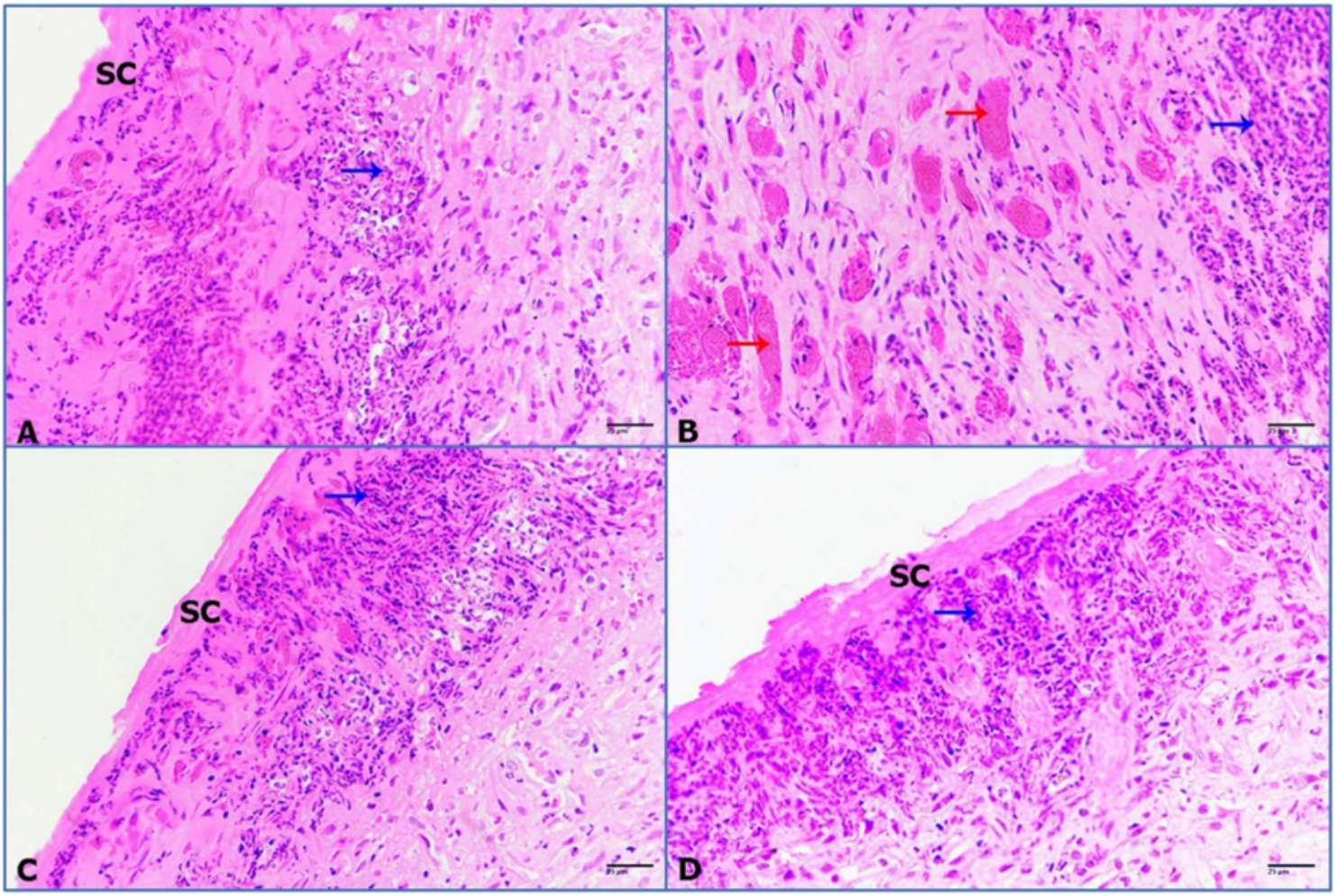

Figure 7

Photomicrographs of rat skin, (red arrows) hemorrhage, (blue arrows) granulomatous reaction. (A) untreated wounded skin, (B) infected untreated wounded skin, (C) infected wound skin treated with Imipenem antibiotic, (D) infected wound skin treated with ZnO-NPs. (HE-400X).

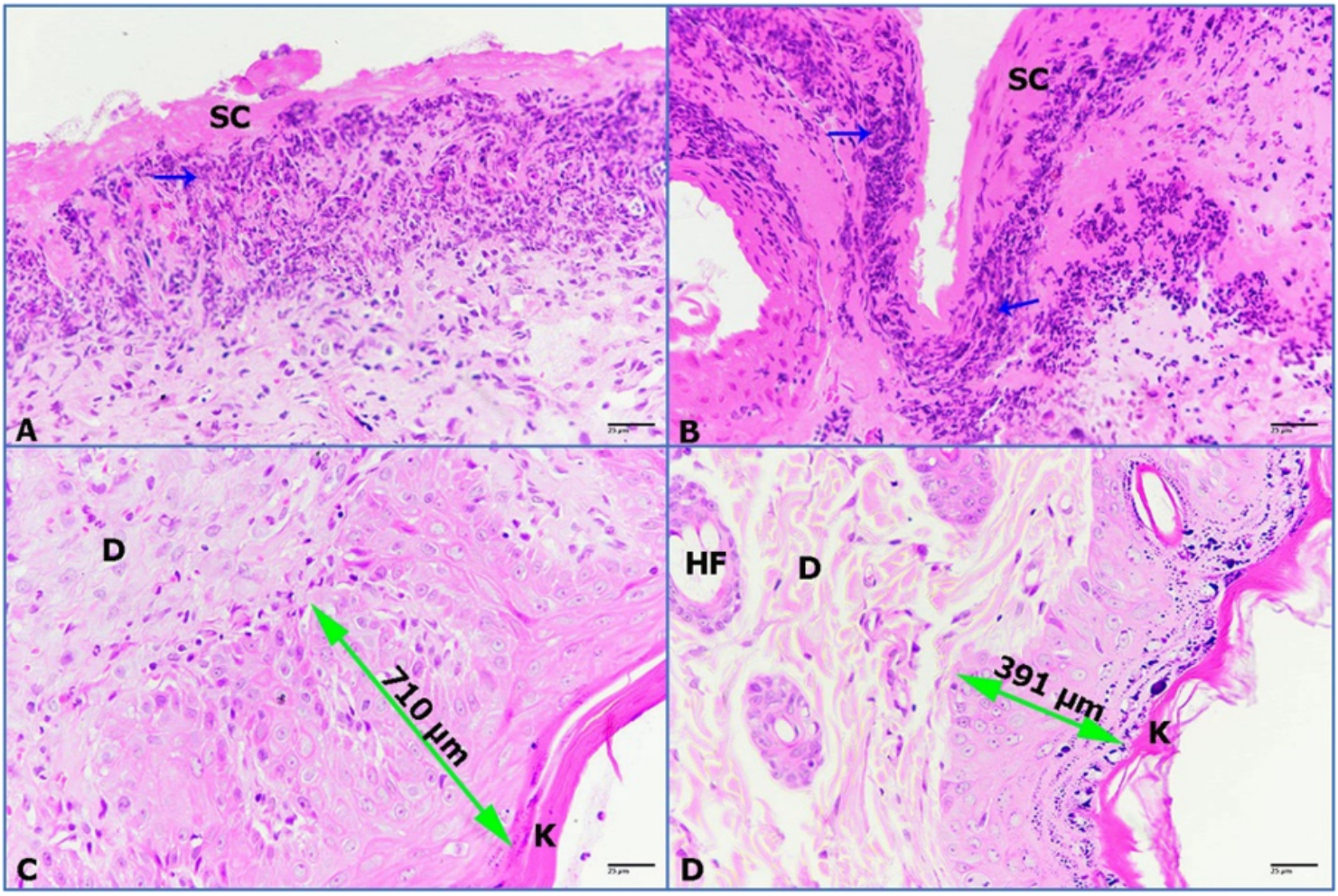

Figure 8

Photomicrographs of rat skin , (K) keratinized layer, (D) dermis, (HF) hair follicle, (double head arrow) regenerated epidermis, (blue arrows) granulomatous reaction. (A) untreated wounded skin, (B) infected untreated wounded skin, (C) infected wound treated with Imipenem antibiotic, (D) infected wound treated with ZnNPs. (HE-400X)

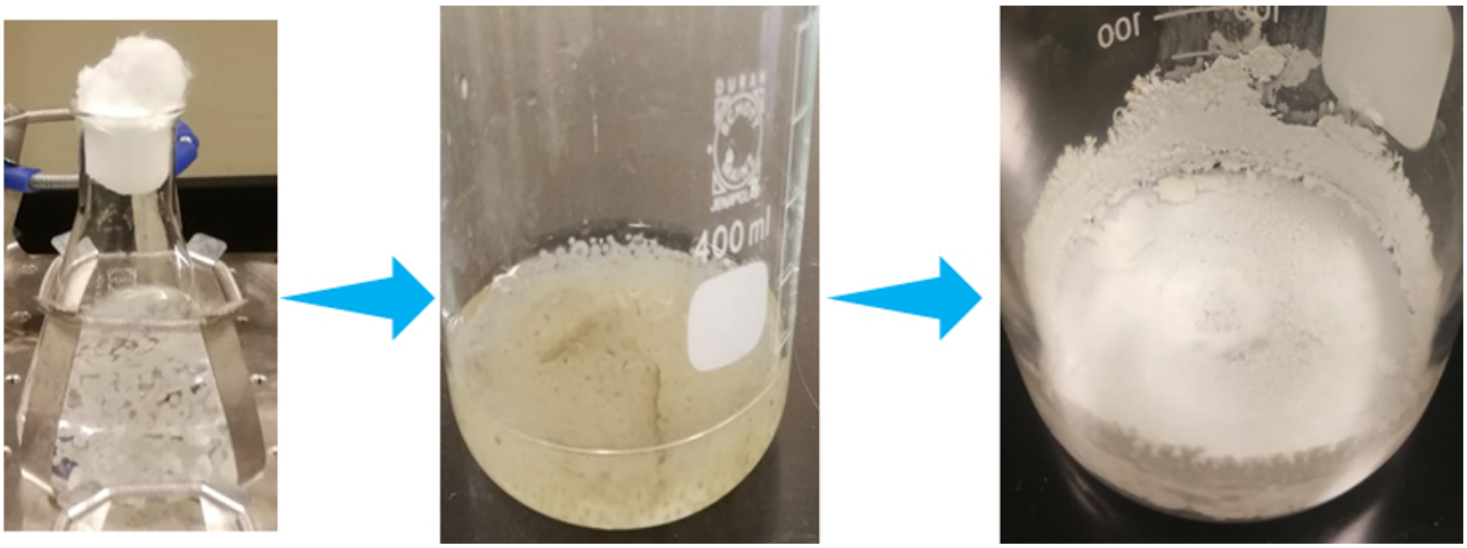

Figure 9

synthesis steps of ZnO-NPs by using Aspergillus niger

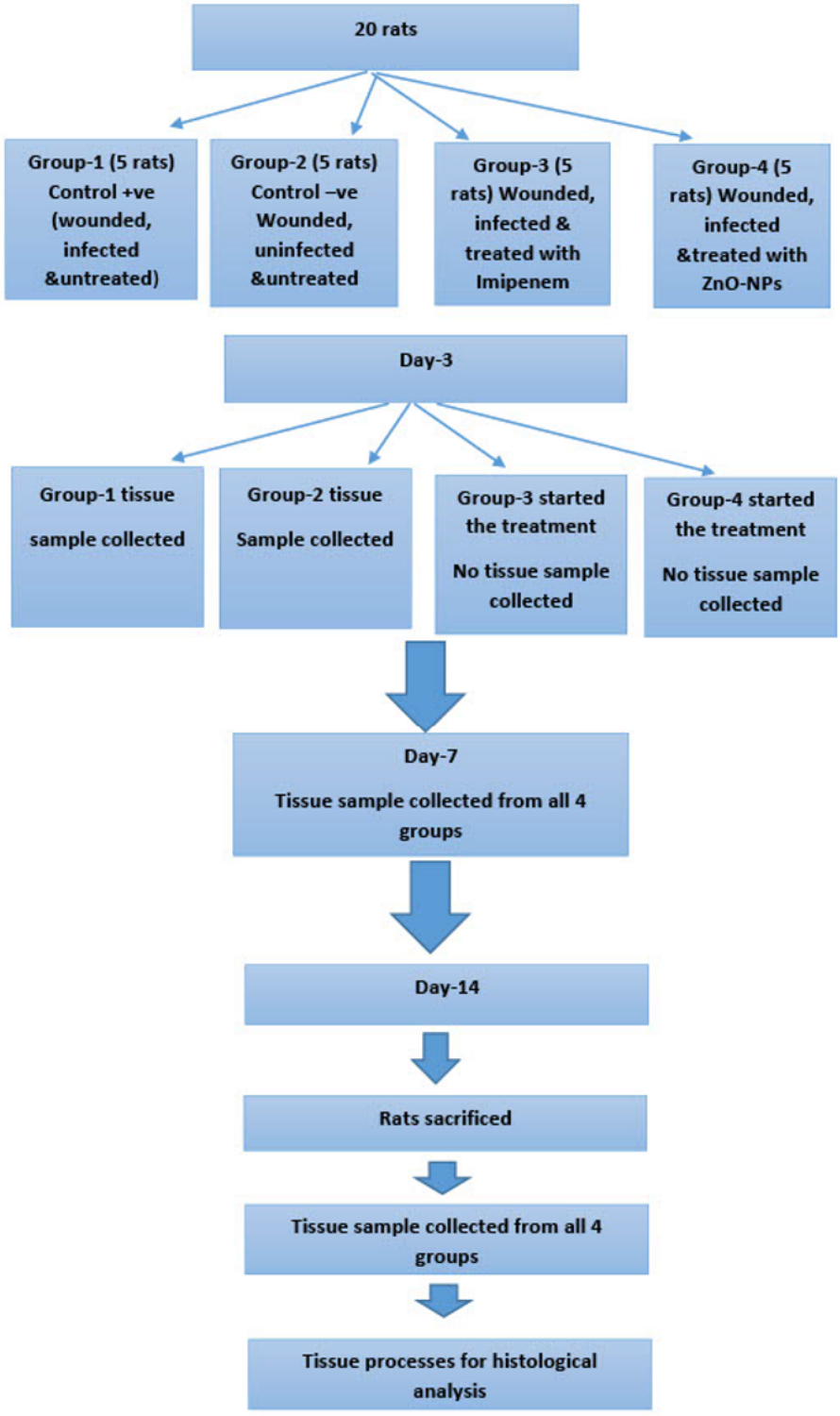

Figure 10

Flow chart showing the experimental design of the four tested rats groups, during the 14 days of wound healing process